

# Poly(2-oxazoline)-Based Microgel Particles for Neuronal Cell Culture

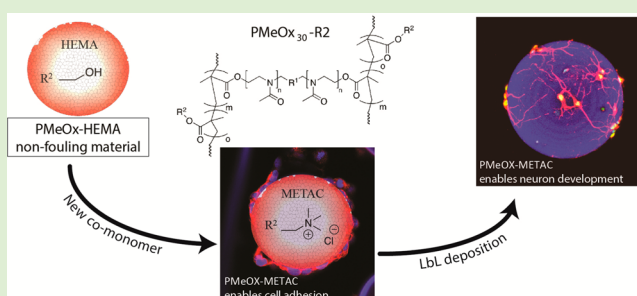
Mitja Platen,<sup>†</sup> Evelien Mathieu,<sup>†</sup> Steffen Lück,<sup>‡,§</sup> René Schubel,<sup>‡,§</sup> Rainer Jordan,<sup>\*,†,‡,§</sup> and Sophie Pautot<sup>\*,†</sup>

<sup>†</sup>Center for Regenerative Therapies Dresden, Technische Universität Dresden, Fetscherstraße 105, 01307 Dresden, Germany

<sup>‡</sup>Professur für Makromolekulare Chemie, Department Chemie, Technische Universität Dresden, Mommsenstraße 4, 01069 Dresden, Germany

<sup>§</sup>Dresden Initiative for Bioactive Interfaces & Materials, Technische Universität Dresden, Mommsenstraße 4, 01069 Dresden, Germany

**ABSTRACT:** An increasing number of *in vivo* and *in vitro* neuro-engineering applications are making use of colloidal particles as neuronal cell carriers. Recent studies highlight the shortcomings of commercial glass particles and stress the benefit of using soft microgel particles (MGPs) instead. This study describes first the fabrication of MGPs from telechelic poly(2-methyl-2-oxazoline)s (PMeOx) cross-linkers and hydrophilic neutral (hydroxyethyl)methacrylate (HEMA) or charged 2-methacryloxyethyltrimethylammonium (METAC) monomers by emulsion polymerization, and it discusses their ability to support cell growth. It establishes that uncharged copolymers lead to MGPs with nonfouling properties inappropriate for cell culture, and it provides a protocol to amend their surface properties to enable cell adhesion. Finally, it demonstrates that the introduction of positive charges by METAC is necessary to obtain surface properties suitable for neuronal cell development. Through the optimization of the PMeOx<sub>30</sub> MGP properties, this work provides general guidelines to evaluate and tune MGP chemistry to obtain microcarriers for neuro-engineering applications.



## 1. INTRODUCTION

The first cross-linked polymer particles were produced in 1935.<sup>1</sup> Since then, MGPs have come to play a central role in a wide range of fields including shear thinning agent for paints,<sup>2</sup> ink jet printing,<sup>3</sup> ceramics engineering, as drug delivery vehicles in the pharmaceutical industry,<sup>4–7</sup> the food industry, and biotechnologies.<sup>8–11</sup> MGPs not only present all the properties of solid colloidal particles such as high surface area, good surface coating properties, and spontaneous assembly properties, but they can also be engineered to have unique chemical and mechanical characteristics, with responsiveness to external triggers,<sup>7</sup> and controlled degradability.<sup>12</sup> Recent improvements in emulsification processes have enabled the fabrication of large micrometer sized particles with surface areas large enough to accommodate cells, and a variety of shapes.<sup>13–18</sup> This makes colloids particularly attractive for neuronal cell cultures, as they allow the relocalization of differentiated neurons without having to resort to enzymatic dissociation typically associated with high cell mortality. Hence, MGPs provide a portable three-dimensional growth matrix on/through which neuronal cell progenitors (NPCs) can grow for several days and where they can be treated to reach the differentiation stage required for the targeted applications.<sup>19–21</sup> MGPs have been typically used in tissue engineering applications to encapsulate molecular or cellular cargo. However, for neuronal cell transplantation and neuro-engineering applications, it is best to grow NPCs on the surface

of the MGPs to prevent that neuronal processes from getting entangled within the polymer matrix;<sup>22</sup> it eases cell migration and cell–cell contact, which is essential for functional integration in a neuronal circuit *in vivo* and *in vitro*. Recent work carried out with poly(*N*-isopropylacrylamide) (PNIPAAm) MGPs<sup>21</sup> illustrated how responsive MGPs improved neuron transplantation in young adult rat hippocampi. Unfortunately, PNIPAAm has unproven biocompatible properties, and these MGPs are not degradable under mild or even physiological conditions. For optimum usage in neuro-engineering, it would be highly desirable to develop MGPs with polymers that are responsive, biocompatible, have adjustable mechanical and chemical properties, and can be biodegradable.

Poly(2-oxazoline)s (POx) are unique in this respect. The polymer offers high structural and property control to specifically tailor MGPs in all the desired properties. POx are prepared by living cationic ring-opening polymerization (LCROP) of 2-substituted-2-oxazolines resulting in polymers of low molar mass distribution<sup>23</sup> and high structural definition. Depending on the 2-substitution, the water-solubility can be adjusted from highly hydrophilic (poly(2-methyl- or 2-ethyl-2-oxazoline)) to highly hydrophobic (e.g., 2-nonyl-),<sup>24</sup> and the polymer pendant groups

Received: December 30, 2014

Revised: March 17, 2015

Published: March 25, 2015

can be used to introduce functional groups for chemical ligation.<sup>25–28</sup> The use of plurifunctional initiators or block copolymers gives access to a broad range of polymer architectures<sup>29</sup> like star-polymers<sup>30</sup> or molecular brushes.<sup>31</sup> Additional features of POx-based hydrogels were extensively reviewed by Wiesbrock and co-workers<sup>32</sup> and recently by Schubert et al.,<sup>33</sup> and include thermoresponsive,<sup>34</sup> pH- and reductive-responsive,<sup>35</sup> or degradable<sup>12</sup> networks. Poly(2-methyl-2-oxazoline) (PMeOx) and poly(2-ethyl-2-oxazoline) are promising candidates for tissue engineering and medical application, as they were found to be nontoxic,<sup>36,37</sup> showed low to no complement activation,<sup>38,39</sup> sufficient stability under physiological conditions,<sup>40,41</sup> a fast renal excretion,<sup>42</sup> and the so-called “stealth effect”.<sup>37</sup>

In this study, we describe the incremental steps necessary to tune the polymer matrix of biocompatible PMeOx<sub>30</sub> to convert their native nonfouling surface into a surface suitable for mammalian cell culture. We show that native MGPs formed from PMeOx<sub>30</sub> cross-linkers and a hydrophilic and neutral HEMA monomer have nonfouling properties that can be medicated by electrostatic deposition of an additional polymer coating to allow human embryonic kidney (HEK) cell adhesion and growth. We explore the effect of the polymer cross-linker density toward shell deposition and cell adhesion, and show that MGPs with high cross-linking density are better suited for cell culture. However, surface modification of PMeOx<sub>30</sub>-HEMA MGPs remains inadequate to allow long-term neuronal cell development. Thus, we explore the benefits of incorporation of a positively charged monomer, METAC, to optimize the surface properties of the particles. We establish that native PMeOx<sub>30</sub>-METAC MGPs exhibit reduced nonfouling properties as compared to PMeOx<sub>30</sub>-HEMA, allowing nonspecific bovine serum albumin (BSA) binding as well as HEK cell adhesion without the need for additional coatings. Finally we show that, similarly to the PNIPAAm MGPs used for neuron transplantation,<sup>21</sup> additional shell deposition steps are necessary to obtain superior adhesive properties and extensive neuronal cell growth required for tissue engineering applications. To our knowledge, this work constitutes the first comprehensive formulation of POx particles for neuronal cell culture and neuro-engineering applications.

## 2. EXPERIMENTAL SECTION

**2.1. Polymer and MGP Preparation.** All chemicals were purchased from Sigma-Aldrich or Acros, and used as received unless otherwise stated. Poly(2-methyl-2-oxazoline) dimethacrylate (PMeOx<sub>30</sub>) was synthesized by LCROP with the bifunctional initiator trans-1,4-dibromo but-2-ene, 2-methyl-2-oxazoline (MeOx) as the monomer and methacrylic acid as the terminator, according to a procedure described recently<sup>43</sup> with a yield of 83%, a total average degree of polymerization of  $n = 30$ , a number-average molar mass of  $M_n = 2860$  g/mol (GPC) at a dispersity of  $\bar{D} = 1.27$  or  $M_p = 3027$  g/mol (MALDI-ToF-MS) and a degree of methacrylate end group functionalization of  $F = 93\%$  as determined by end group analysis based on <sup>1</sup>H-NMR spectroscopy data.

PMeOx MGPs (PMeOx<sub>30</sub>-HEMA, PMeOx<sub>30</sub>-METAC) were produced either by emulsion redox polymerization (water/dodecane) in batch or in a microfluidic device (water/paraffin) using different ratios of POx as the cross-linker and HEMA or METAC as the monomer and SPAN80 as the surfactant to yield MGPs of different cross-linking densities.

**2.2. Surface Modification.** PMeOx<sub>30</sub>-HEMA as well as PMeOx<sub>30</sub>-METAC beads were treated with iterating layers of poly(allylamine hydrochloride) (PAH) and poly(sodium-4-styrene-sulfonate) (PSS) (Sigma-Aldrich, Germany) as previously described<sup>21</sup> to enable electro-

static deposition of poly(L-lysine) (PLL,  $M_w = 120.000$  g/mol, Sigma-Aldrich) to enable neuronal cell adhesion. The first layer was deposited by incubating the MGPs in PAH solution (PAH,  $M_w = 8000–11\,000$  g/mol, dissolved at 5 mg/mL in potassium acetate), for 25 min on a rolling shaker. The excess PAH was removed by washing the particles three times with distilled water (dH<sub>2</sub>O). The next counterion layer was deposited by incubating the microgel particles in PSS solution (PSS,  $M_w = 70000$  g/mol, 5 mg/mL in potassium acetate) for 25 min on a rolling shaker. Excess PSS was removed by washing the particles three times with dH<sub>2</sub>O. The PAH/PSS deposition cycle was repeated at least three times to obtain the desired negatively charged polymer shell that enables electrostatic adsorption of necessary PLL amounts for robust neuronal cell adhesion on all MGPs. At this stage, the PAH/PSS-coated particles could be stored in water at 4 °C for at least 2 weeks without appreciable changes of their properties. The final PLL coating step was performed 48 h before particles were used for cell culture. The particles were sterilized in 70% ethanol overnight, recharged in borate buffer, and then incubated overnight on a rolling shaker in a PLL solution (5 mg/mL in pH 7.4 PBS). The excess PLL solution was removed, and the particles were then washed three times with PBS. Twelve hours prior to cell seeding, PLL-coated MGPs were incubated in culture medium at 37 °C to allow the medium to fully penetrate the microgel.

**2.3. Surface Assessment.** **2.3.1. Nonspecific Adhesion.** PLL-coated particles were incubated for 30 min, while rotating, with 0.1% BSA (Carl Roth, Germany) in Dulbecco's phosphate-buffered Saline (DPBS); containing 5% FITC-labeled BSA (Sigma-Aldrich, Germany). After sedimentation, the beads were washed three times for 5 min with dH<sub>2</sub>O. The adhesiveness of the particles was determined by confocal microscopy.

**2.3.2. Characterization of the PLL Deposition Process.** To estimate the increase in adsorbed PLL with increased numbers of layer-by-layer deposition cycles, we labeled the accessible primary amine of the deposited PLL with a fluorescent tracer. After each new deposition cycle, a small amount of particles was set aside and was coated with PLL. The PLL-coated MGPs were then suspended in 0.2 M borate buffer (pH 7.4) and left to equilibrate for at least 15 min. The labeling reaction was started by adding Alexa 555-NHS ester, a small diffusible fluorescent dye carrying a reactive succinimidyl ester group (Life Technologies; 10 mg/mL in dimethyl sulfoxide), to the MGPs suspension following the manufacture recommendations. The number of labeled primary amine groups correlated with PLL concentration. Hence, the measure of the residual fluorescence provided a relative measure of PLL distribution as a function of the number of deposition cycle. The cross-section of the labeled MGPs was imaged by confocal microscopy. To allow the comparison of the fluorescence intensities between samples, we kept the acquisition parameters constant (identical laser power, scanning rate, and detector gain) and imaged them on the same day. For each particle, we measured the averaged radial intensity profile. The amount of deposited PLL for a given number of deposition cycles was determined by averaging the mean radial intensity profile of at least 10 particles.

**2.4. Characterization of MGPs Elastic Properties.** The elastic properties of the MGPs were measured using atomic force microscopy (AFM; Nanowizard BioScience AFM, JPK Instruments AG) at room temperature. Tipless silicon nitride cantilevers with an average force constant of 0.12 N/m were used (NP-O10, Bruker). Ten micrometer glass beads (Gerlinde) were attached to the cantilevers using Araldite Rapid (Huntsman Advanced Materials). Force curves with a trigger point at 2.5 to 3 nN were obtained of beads immersed in DMEM medium (incubated overnight, 100 force curves/bead). The Young's modulus was obtained by fitting the force curves using the Hertzian model for spherical/parabolic indentation (Poisson ratio 0.45).<sup>44</sup>

**2.5. Cell Culture.** **2.5.1. Human Embryonic Kidney Cells.** HEK-293T cells were seeded at a density of 25 000 cells per well into 12-well plates (Greiner Bio-One) containing a thin layer of PLL-coated beads and incubated for 3 to 7 days in DMEM supplemented with 2 mM L-glutamine, 100 unit/mL penicillin, 100 mg/mL streptomycin, and 10% FBS (Life Technologies – Invitrogen, Germany).

**2.5.2. Primary Neurons.** Hippocampal neuronal cells from embryonic rat were harvested 18 days postfertilization (embryonic day 18, E18) following standard procedures. The cells were seeded in a

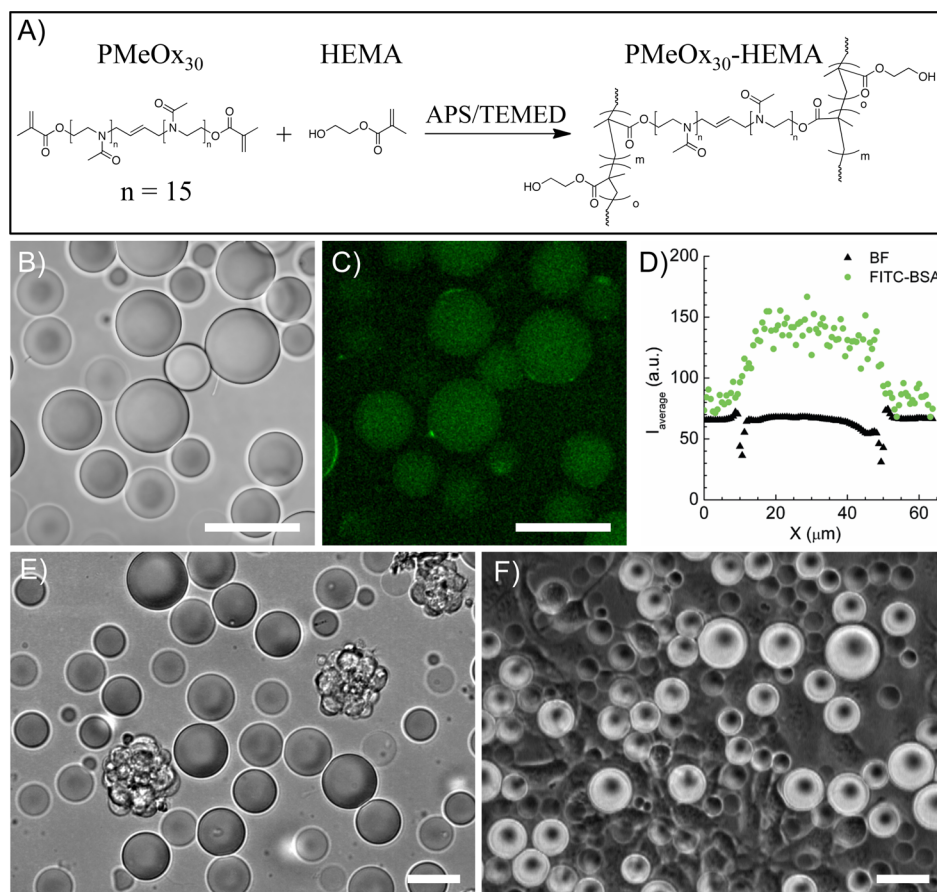


**Figure 1.** Native PMeOx<sub>30</sub>-HEMA MGPs. (A) Reaction scheme of PMeOx<sub>30</sub>-HEMA MGPs synthesis by emulsion polymerization. (B) Bright field microscopy image of the resulting microgel particles (MGPs). (C) Examination of the nonspecific FITC-BSA adsorption on native MGPs. (D) FITC-BSA intensity profile (green circle) taken across the equatorial plane of MGPs; the position of the particle edge was determined using the corresponding bright field profile (black triangle). FITC-BSA fluorescence intensity decreased at the edge, indicating that BSA did not adsorb to the MGPs. (E) E18 hippocampal cells did not interact with native MGPs and formed independent neuronal cell clusters. (F) Native MGPs seeded on a HEK-293 cell monolayer sat on the top of the cells without signs of interaction with the cells. Scale bars = 50  $\mu\text{m}$ .

12-well plate at a density of 100 000 cells per well and kept at 37 °C and 5% CO<sub>2</sub> for 3 to 7 days. Each well contained a thin layer of coated particles pre-equilibrated in cell culture medium. The MGPs were slightly denser than water and thus settled at the bottom of the dish. Yet, they were not as dense as glass particles and thus they required extra care not to aspirate MGPs during liquid handling and washing steps. The medium was composed of Neurobasal (Gibco) with Serum-Free Supplement B-27 (1 mL per 50 mL), 200 mM L-glutamine, 2 units/mL of penicillin and 2  $\mu\text{g}/\text{mL}$  of streptomycin. All cell culture reagents were purchased from Life Technologies. Culture growth was assessed each day by means of bright field microscopy (Axiovert 25 microscope, Zeiss and ProgRes C10plus camera).

**2.6. Staining.** Cultured cells, on MGPs or coverslips, were gently washed with PBS, fixed with 4% paraformaldehyde for 20 min and washed again with PBS (three times for 5 min). Cells were permeabilized in 5% normal goat serum (NGS, Gibco, USA), 0.1% BSA (Roth, Germany) and 0.3% Triton X 100 (Fluka, USA) for 1 h. Afterward, the samples were incubated with the first antibody in 5% NGS and 0.1% BSA for 1 h. After washing (3 $\times$  PBS, 5 min), the secondary antibody diluted in 5% NGS and 0.1% BSA was added for 1 h. Finally, cells were washed three times for 5 min with dH<sub>2</sub>O.

The following primary antibodies were used: Nestin, 1:700 (Millipore, USA), Neuronal Class III  $\beta$ -Tubulin, 1:1000 (Covance, Germany), and Alexa Fluor 546 phalloidin (Invitrogen). The following secondary antibodies were used: Alexa Fluor 488, antimouse, 1:500 and Alexa Fluor 555, antirabbit, 1:500 (Invitrogen, Germany).

### 3. RESULTS

#### 3.1. Properties of the Native PMeOx<sub>30</sub>-HEMA Particles.

We first prepared MGPs from the telechelic PMeOx<sub>30</sub> cross-linker and HEMA as the monomer at a weight ratio of 30:70 (Figure 1A) by emulsion polymerization in batch. The resulting particles were sieved through a 250  $\mu\text{m}$  mesh-strainer to remove macroscopic particles, and through a 30  $\mu\text{m}$  mesh-strainer to obtain MGPs with particle diameters in the range of 30 to 250  $\mu\text{m}$ . We discarded particles smaller than 30  $\mu\text{m}$ , as they do not offer a surface large enough to accommodate neuronal processes. As previous studies on glass particles showed that the dominant signaling cues for neuron maturation were provided by the composition of cell culture medium and not by the size of the particles.<sup>19,20</sup> No further action was taken to control MGPs size distribution. A bright field image of the PMeOx<sub>30</sub>-HEMA (30:70) MGPs is shown in Figure 1B. BSA has a high adhesive affinity to both hydrophilic and hydrophobic surfaces and thus is often used as a nonspecific surface blocking agent. To evaluate the nonfouling properties of these MGPs, we measured the nonspecific adsorption of BSA onto the native particles. MGPs were incubated for 30 min in PBS containing fluorescently labeled BSA, and washed three times before imaging the resulting FITC-BSA spatial distribution using confocal fluorescence microscopy (Figure 1C). The particles showed a weak fluorescent signal brighter at the particle core indicating that

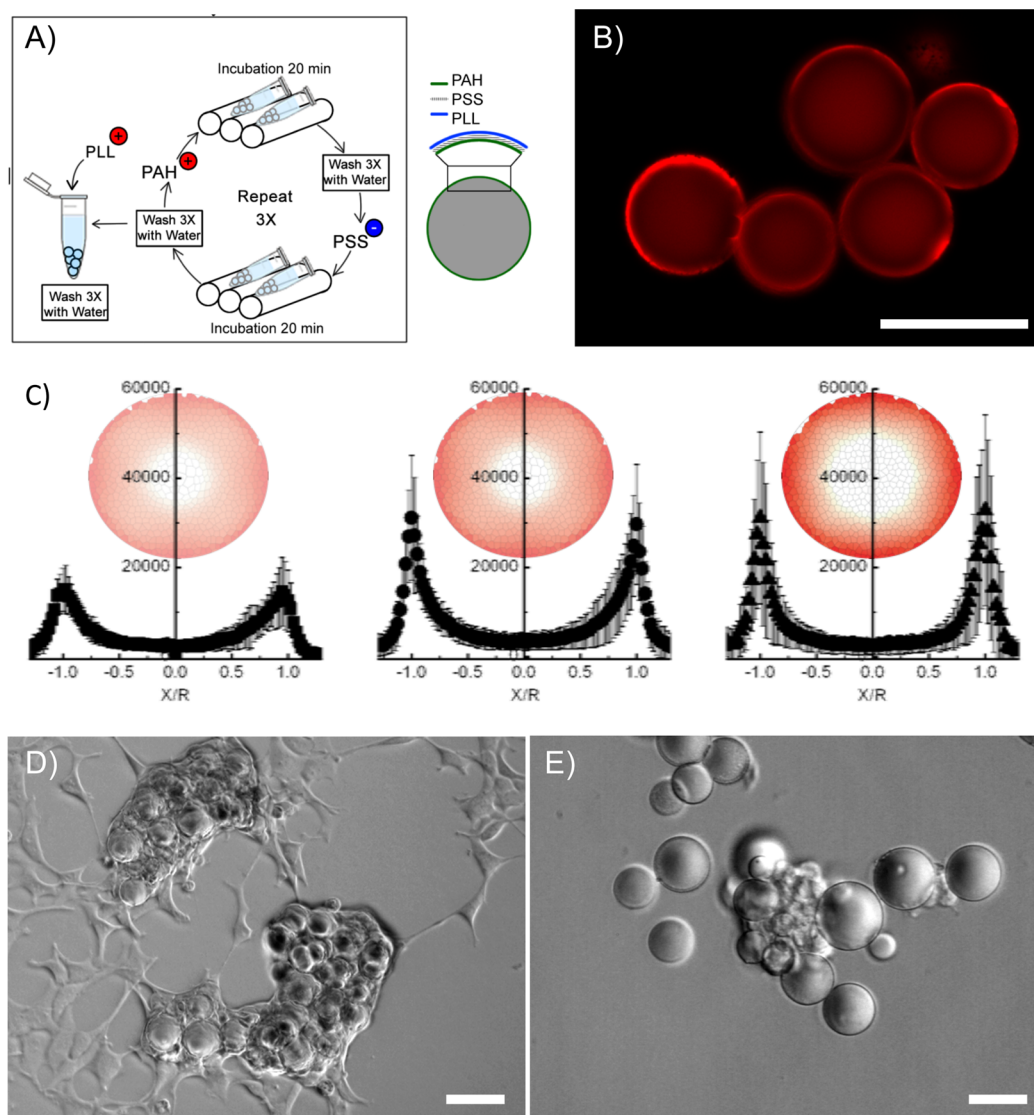


**Figure 2.** Surface modification of PMeOx<sub>30</sub>-HEMA MGPs. (A) Scheme of LbL deposition (PAH and PSS) to improve cell adhesion. (B,C) Characterization of PLL distribution, after LbL deposition, using Bodipy. (B) Laser scanning confocal microscopy of the equatorial plane of a PLL coated MGP. (C) Changes in PLL distribution with increasing number of deposition cycles (0, 2, and 4 cycles). Averaged Bodipy intensity profile taken across the equatorial plane of MGPs; as the number of cycles increased, less PLL penetrated the MGPs, and more was deposited on the surface. (D,E) Results of PLL coating toward cell adhesion. (D) HEK cells engulfed PLL-coated MGPs within 48 h. (E) E18 hippocampal cells showed partial interaction with PLL-coated MGPs. Scale bars = 50  $\mu\text{m}$ .

the pores of the polymer network were sufficiently large to allow diffusion of labeled BSA into the MGPs. Bright patches at the surface of some particles indicated the presence of surface irregularities not directly appreciable by bright field microscopy. To determine whether BSA was retained on the MGP surface, we measured the fluorescence intensity profile of FITC-BSA at the particle equatorial plane of the MGPs (Figure 1D). The edge of the particles was determined from the corresponding bright field intensity profile (Figure 1D; black triangle). For all particles we observed a dumbbell shaped intensity distribution of FITC-BSA (green circle) that faded out at the edge of the particle, suggesting the outward diffusion of the loaded BSA from the porous matrix during the washing steps. No increase in fluorescent intensity was observable at the edge of the particle, indicating that FITC-BSA did not adsorb on the particle surface except at random spots on a few particles. These observations suggested that native PMeOx<sub>30</sub>-HEMA MGPs exhibit minimal nonspecific adhesion of BSA.

Next, we examined the affinity of mammalian cells for the native surface of the MGPs. PMeOx<sub>30</sub>-HEMA (30:70) particles were sterilized and pre-equilibrated in culture medium at 37 °C for 12 h prior to their use for cell culture. To maintain a sterile environment, all subsequent steps were carried out in a biosafety cabinet with solutions filtered through a 0.22  $\mu\text{m}$  filter (Acrodisc, Corning Inc.). MGPs were placed in culture dish, and rat primary E18 hippocampal cells were seeded in the dish upon isolation. Over the next days in culture, neuronal cells did not make adhesive contact with the MGPs. Instead, they preferred forming free-floating clusters with each other (Figure 1E). Considering that neurons are notorious for their stringent surface requirements, we repeated this experiment with HEK cells that are known for being less selective toward their growth surface than neuronal cells. MGPs were directly added on a 2D monolayer of HEK cells; after 72 h in culture, cells remained on the culture dish as a monolayer, indifferent to the MGPs (Figure 1F). Even after several days on top of the HEK cell monolayer, MGPs could be

washed away easily. In conclusion, these results indicated that further processing was required to amend native P $\text{MeOx}_{30}$ -HEMA particles nonfouling properties and obtain MGP suitable for adherent cell culture.

**3.2. Particle Coating Strategy to Promote Cell Adhesion.** To promote neuronal cell growth, cell culture surfaces have to be coated with polycationic polymers such as PLL.<sup>45</sup> To deposit PLL on P $\text{MeOx}_{30}$ -HEMA (30:70) without modification of the polymer chemistry, we devised a noninvasive layer-by-layer (LbL) deposition of polyelectrolytes to progressively increase the surface charge of the MGPs to a point where PLL could be electrostatically adsorbed on the MGPs.<sup>21</sup> The procedure is schematically described in Figure 2A. To visualize how the successive deposition cycle of PAH+ and PSS- translate into increasing the amount of PLL deposited, we incubated the particles with small, highly diffusive fluorescent dye carrying a reactive succinimidyl ester group (Experimental Section) that readily penetrated the hydrogel and reacted with accessible primary amines present on PLL to be specifically retained where PLL has been deposited, highlighting its spatial distribution.

The MGPs were extensively washed to remove non-cross-linked dye before we visualized the fluorescence of the dye cross-linked to the adsorbed PLL by laser scanning confocal microscopy (Figure 2B). We measured the fluorescence intensity profile for each particle. The mean radial intensity profile for a given number of deposition cycles was obtained by averaging the radial intensity profiles normalized by the particle radius of at least 10 particles (Figure 2C). When PLL was deposited on native MGPs ( $c = 0$ ) we observed a weak fluorescence signal across the MGPs diameter, indicating that PLL ( $M_w = 120\,000$  g/mol) could diffuse into the P $\text{MeOx}_{30}$ -HEMA (30:70) MGPs with a higher concentration at the edge of the particle due to a combination of diffusion and adsorption. As we increased the number of deposition cycles (0, 2, 4), the fluorescent tracer provided a sharper definition of the MGPs edge and a lower fluorescent intensity at the center of the particle, indicating that less PLL could diffuse into the particles, and more was deposited on the surface.

To assess the benefit of PLL deposition toward cell adhesion, we repeated the previous experiment and placed PLL coated P $\text{MeOx}_{30}$ -HEMA (30:70) MGPs on a monolayer of HEK cells in culture. Bright field imaging showed that, after 2 days, HEK cells engulfed the particles (Figure 2D), indicating that the cells were successfully drawn to leave their 2D culture dish and to preferentially adhere on the PLL coated MGPs. However, rat primary E18 hippocampal cells directly seeded on PLL coated MGPs showed only marginal signs of interactions. Neuronal cells remained preferentially clustered with each other (Figure 2E), suggesting that the particle properties should be further modified to obtain a surface suitable for neuronal cell adhesion.

**3.3. Properties of P $\text{MeOx}_{30}$ -HEMA MGPs of Different Compositions.** BSA and PLL diffusion into MGPs suggested that P $\text{MeOx}_{30}$ -HEMA (30:70) particles were highly porous, which, combined with a crude emulsification process, could lead to heterogeneous surface properties and explain the difficulty to create a satisfactory polymeric shell by LbL deposition for cell adhesion. To obtain more homogeneous particles, diminish surface defects, and improve the shell deposition process, the initial emulsion polymerization was performed with a microfluidic device. To further improve particle surface properties, we increased the polymeric matrix cross-linking density. MGPs with varied P $\text{MeOx}_{30}$  and HEMA ratios (50:50) and (70:30) were

produced, and the resulting particles were treated as previously described. As expected, the MGPs obtained were more uniform in size with significantly less macroscopic defects (Figure 3A-B). Please note that MPGs prepared with more telechelic P $\text{MeOx}_{30}$  cross-linker resulted in stiffer MGPs.<sup>43</sup> The Young's modulus as determined by AFM for P $\text{MeOx}_{30}$ -HEMA (50:50) and P $\text{MeOx}_{30}$ -HEMA (70:30) was  $13.2 \pm 2.4$  kPa and  $21.8 \pm 6.5$  kPa, respectively.<sup>43</sup> When we assessed nonspecific BSA adsorption on the native particles, we observed no signs of changes in the surface interactions. The FITC-BSA fluorescence intensity profile normalized by the particle radius showed that BSA was still penetrating the polymer matrices of these MGPs; however, differences in BSA distribution were noticeable (Figure 3C). The washing steps resulted in a decrease in fluorescence at the edge of all particle types, indicating that BSA could diffuse outward of all three P $\text{MeOx}_{30}$ -HEMA matrices produced. This decrease in fluorescence intensity was comparable for both (70:30 down triangle) and (50:50 up triangle), but it was less pronounced for (30:70 circle), indicating that BSA diffused out slower from highly cross-linked particles. These observations confirmed that increasing the cross-linker density led to a decrease in porosity of the polymeric hydrogel matrix. MGPs were then coated and we measured the resulting PLL distribution for native particles and MGPs that underwent five-deposition cycles ( $c = 5$ ) of PAH+ and PSS-. Figure 3D shows the resulting fluorescence intensity profile. The edge of (50:50) and (70:30) P $\text{MeOx}_{30}$ -HEMA MGPs displayed an identical sharp fluorescent peak, indicating that after five-deposition cycles a comparable amount of PLL had been deposited for both cross-linking density. The edge of P $\text{MeOx}_{30}$ -HEMA (30:70) displayed a significantly brighter peak; the aspect ratio between peak maximum and peak waist as well as the brighter core of the MGPs suggested that the difference in intensity could be attributed to the penetration of PLL in the porous P $\text{MeOx}_{30}$ -HEMA (30:70) MGPs.

When we examined HEK cell adhesion on the coated particles by immuno-cytochemistry using DAPI as the nuclear marker, and phalloidin as the F-actin marker, we observed an extensive colonization of the particle surface by HEK cells on both P $\text{MeOx}_{30}$ -HEMA MGP types after 3 days. Confocal images of the MGPs equatorial plane showed that HEK cells were distributed all around the particle surface (Figure 3E,F). When we examined the growth of rat primary E18 hippocampal cells on these particles after 3 days, we were able to observe a very small number of neuronal cells attached and differentiated. Confocal imaging of immuno-cytochemistry stains revealed that neurons positive for Tuj-1 were present on the particle surface, indicating that these large particles could support neuronal cell development albeit with a low success rate since most particles did not bare any cells (Figure 3G,H). These results suggested that the P $\text{MeOx}_{30}$  particle's nonspecific adhesive properties were set for a given composition. The increase of the MGP cross-linking density resulted in an improved LbL deposition that allowed adhesion of a few neuronal cells poorly developed. After a week in culture, the cell population counted  $57\% \pm 7$  Tuj-1 positive cells,  $20\% \pm 1.4$  nestin positive cells, 10% of apoptotic cells, and  $14\% \pm 2$  of cells double positive for nestin and Tuj-1, suggesting a slow neuronal differentiation on PLL coated P $\text{MeOx}_{30}$ -HEMA carriers in differentiation culture medium.

**3.4. Introducing Charges by METAC Monomers to Improve Neuronal Cell Adhesions.** To further improve neuronal cell adhesion and differentiation, we substituted the hydrophilic and neutral HEMA by positive METAC to

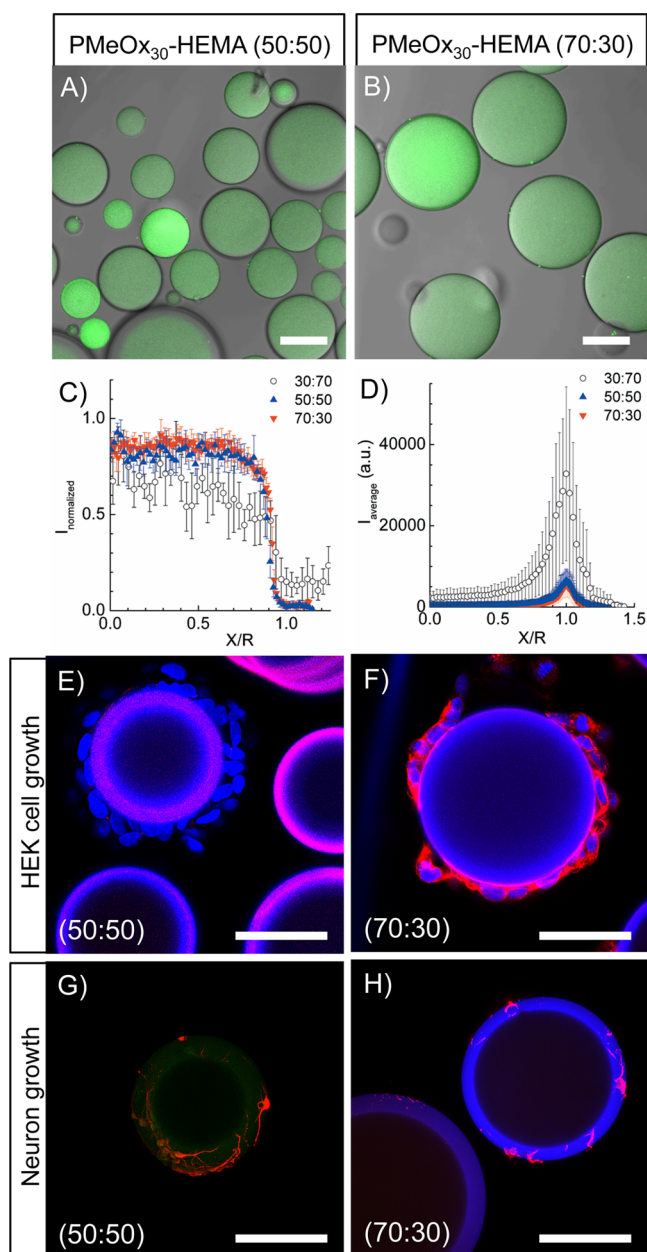


**Figure 3.** Comparison of PMeOx<sub>30</sub>-HEMA particles with different cross-linking densities (50:50 and 70:30). (A,B) Combined transmission and laser scanning confocal microscopy fluorescence images of the equatorial plane of MGPs loaded with FITC-BSA. (C) Comparison of the average radial distribution of FITC-BSA for the three cross-linking densities: (30:70 open circle; 50:50 blue up-triangle; 70:30 red down-triangle). (D) Comparison of the average radial distribution of labeled PLL for three cross-linking densities (30:70 open circle; 50:50 blue up-triangle; 70:30 red down-triangle) after five deposition cycles. (E,F) HEK cell adhesion on 50:50 and 70:30 PMeOx<sub>30</sub>-HEMA MGPs. Laser scanning confocal microscopy images of one Z-section taken at the equatorial plane of MGPs; HEK cells stained for DAPI (blue) and phalloidin (red) after 7 days in culture. (G,H) Adhesion and differentiation of E18 neuronal cells on 50:50 and 70:30 PMeOx<sub>30</sub>-HEMA MGPs. Laser scanning confocal microscopy images of one Z-section taken at the equatorial plane of MGPs; neuronal cells stained for DAPI (blue) and Tuj-1 (red) after 7 days in culture. Scale bars = 100 μm.

systematically introduce a net charge into the MGPs (Figure 4A). Since high cross-linking density improved the LbL deposition, particles with a 70:30 PMeOx<sub>30</sub>-METAC ratio were produced.

With METAC as the comonomer, the MGPs were found to be significantly softer; for PMeOx<sub>30</sub>-METAC (70:30) a Young's modulus of only  $5.6 \pm 1$  kPa was determined by AFM.<sup>43</sup> To assess the surface properties, the native particles were incubated with labeled-BSA and then washed before imaging. Confocal imaging of the particles after 4 h in water showed a bright core corresponding to the loaded BSA, and a decrease in fluorescent closer to the edge due to the outward diffusion of BSA during the washing steps. Yet, a strong fluorescence signal remained at the edge of the particle due to the nonspecific BSA adsorption on the particle surface (Figure 4B). The fluorescence intensity profile taken through the particle equatorial plane (Figure 4C) confirmed that FITC-BSA was retained on native PMeOx<sub>30</sub>-METAC, confirming that the introduction of positive charges by METAC enabled us to medicate PMeOx<sub>30</sub> MGPs native nonfouling properties.

To determine whether the polymeric shell deposition remained necessary to promote cell adhesion, we seeded HEK cells on either uncoated ( $c = 0$ ) or PLL coated ( $c = 1$ ) PMeOx<sub>30</sub>-METAC particles. After 2 days, cells attached to the particles were fixed and stained with phalloidin and DAPI. Confocal imaging of these samples revealed no significant differences in HEK cell morphology. Cells were spreading with visible focal adhesion points, even on uncoated MGPs (Figure 4D), suggesting that the cationic charges introduced with METAC are sufficient to promote HEK cell adhesion. However, neuronal cells failed to adhere and grow on uncoated particles (data not shown). As a result, we prepared two series of PMeOx<sub>30</sub>-METAC particles: one that underwent a single deposition cycle ( $c = 1$ ) followed by PLL coating (Figure 4F–H) and another that underwent five-deposition cycles ( $c = 5$ ) again, followed by PLL coating (Figure 4I–K). Bright field images showed that more neuronal cells adhered to the particles with more deposition cycles (Figure 4I). Confocal fluorescence imaging of immunostained particles showed that few neuronal cells adhered to  $c = 1$  particles. Their neuronal processes stained with Tuj-1 remained underdeveloped, as it is typically observed for NPCs (Figure 4G). However, nestin expression in these cells was low (Figure 4H), suggesting that these cells are no longer NPCs but slow differentiating neurons. In comparison, confocal fluorescence imaging of neuronal cells seeded on  $c = 5$  particles showed a high density of long and bright Tuj-1 positive processes (Figure 4J) and a distinct strongly nestin positive cell population (Figure 4K), indicating the coexistence of a population of differentiating neurons with a population of NPCs similar to PLL-coated glass particles.<sup>19</sup> After a week in culture the cell population was composed of more than  $73\% \pm 8$  Tuj-1 positive cells (92% of which were mature NeuN positive neurons),  $26\% \pm 5.7$  nestin positive cells,  $2\% \pm 1.5$  GFAP positive cells, and no apoptotic cells on the MGPs, suggesting that there was no difference between neuronal development on PLL coated glass or PNIPAAm particles, and PLL-coated PMeOx<sub>30</sub>-METAC carriers in differentiation culture medium. In summary, these results indicated that although it was not necessary to coat PMeOx<sub>30</sub>-METAC particles to promote HEK growth, LbL deposition and final PLL coating tremendously improved neuronal cell adhesion, growth, and maturation.

#### 4. DISCUSSION

In this study, we explored the link between PMeOx microcarrier composition and their ability to support neuronal cell culture. PMeOx<sub>30</sub>-based microcarriers with different comonomers were successfully produced using an emulsion polymerization in batch

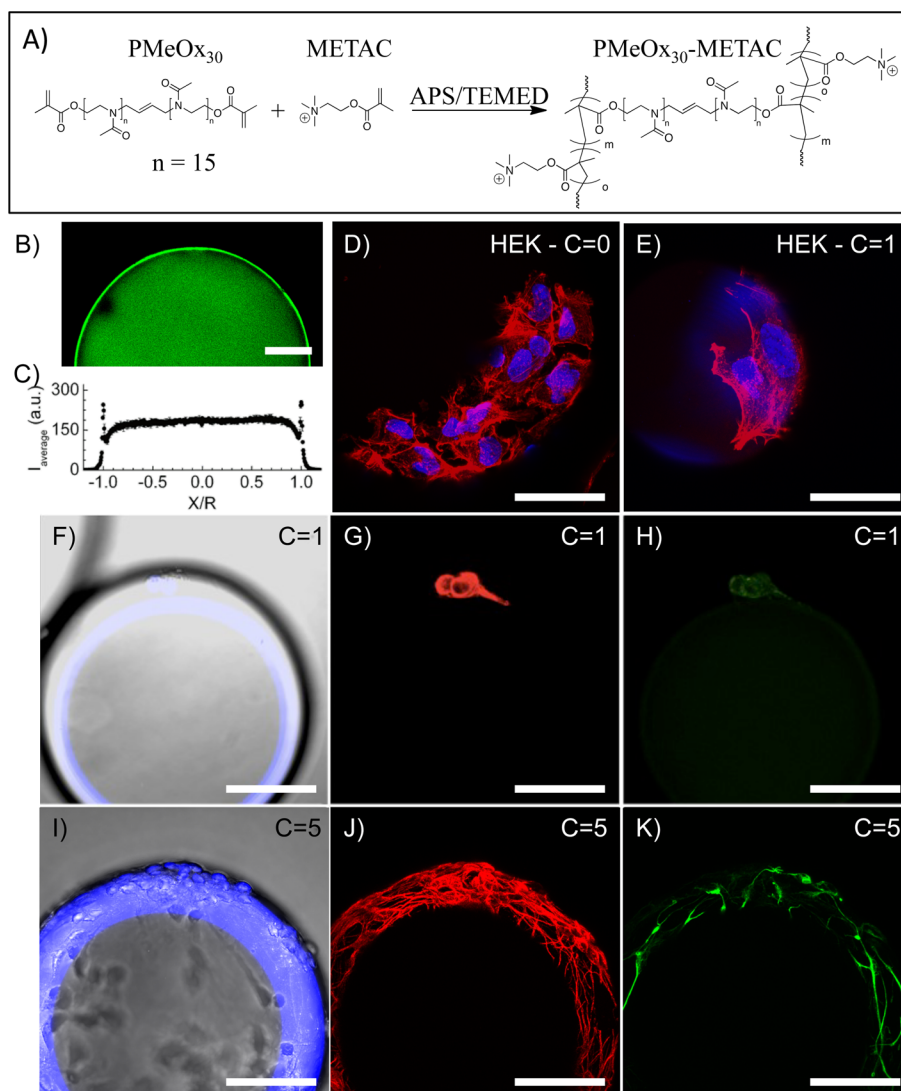


**Figure 4.** PMeOx<sub>30</sub>-METAC with improved neuronal cell growth. (A) Reaction scheme of the PMeOx<sub>30</sub>-METAC MGP synthesis. (B) Laser scanning confocal microscopy image of one Z-section taken at the equatorial plane of uncoated PMeOx<sub>30</sub>-METAC MGP incubated in FITC-BSA (green). (C) Averaged fluorescence intensity distribution of FITC-BSA across the particle 4 h after loading. The fluorescence intensity increased sharply at the edge of the particle indicating nonspecific adsorption of FITC-BSA on the MGPs. (D,E) HEK cell adhesion studies of PMeOx<sub>30</sub>-METAC particles. HEK cells labeled with a nuclear marker, DAPI (blue), and actin (red) on uncoated MGPs (D), and PLL coated MGPs after one deposition cycle  $c = 1$  (E). (F–K) Adhesion and differentiation of E18 neuronal cells on PMeOx<sub>30</sub>-METAC MGPs. Ten frames of a Z-stack series obtained by laser scanning confocal microscopy were projected on the XY plane; neuronal cells stained for DAPI (blue), Tuj-1 (red), and nestin (green) after 7 days in culture. MGPs coated with PLL after one deposition cycle ( $c = 1$ ) (F–H), and for MGPs coated with PLL after five deposition cycles ( $c = 5$ ) (I–K). Scale bars = 50  $\mu\text{m}$ .

or in a microfluidic device. Native PMeOx<sub>30</sub>-HEMA MGPs exhibited nonfouling properties, which prevent sufficient cell adhesion. Two approaches were used to amend their native nonfouling properties and enable cell culture applications: coating of the particle surfaces and changes in polymer composition. We first demonstrated that by coating PMeOx<sub>30</sub> MGP with an adhesion promoting shell by LbL deposition, we could promote cell growth on soft MGPs regardless of the MGP native properties. Then, we showed that increasing the MGP cross-linking density improved the quality of the polymeric shell as demonstrated by the cell culture results. However, the poor development of neuronal cells on coated PMeOx<sub>30</sub>-HEMA particles denoted that MGPs surface chemistry had to be further tailored to satisfy specific cell-type needs. Since the quality and/or efficiency of the LbL treatment is dependent on two factors: (1) the initial nonfouling property of the polymeric microgel particles, and (2) the initial net surface charge carried by the

particle, we prepared PMeOx MGPs with a charged comonomer. The introduction of positive charges significantly improved native PMeOx<sub>30</sub>-METAC MGPs quality for HEK cell culture. However, this remained insufficient for neuronal cell adhesion. Similarly to PNIPAAm MGPs, an additional polymeric shell deposition was mandatory to obtain robust neuronal cell development on PMeOx<sub>30</sub>-METAC MGPs.

## 5. CONCLUSION

This work surveyed the key physical properties required to obtain PMeOx<sub>30</sub> MGP suitable for neuron-engineering applications and highlighted the need to further optimize the hydrogel particle composition to develop native MGPs readily suitable for neuronal cell culture. Results showed that after shell deposition, PMeOx-METAC MGP performed as well as PNIPAAm MGPs used for neuron transplantations.<sup>21</sup> Extensive formulation and

evaluation work still lies ahead to fully take advantage of the functional substitutions available with POx polymers and incorporate the versatility of POx properties such as their thermosensitivity<sup>46,47</sup> and biodegradability<sup>43</sup> for neuro-engineering applications.

## AUTHOR INFORMATION

### Corresponding Authors

\*E-mail: Pautot.crtdd@gmail.com.

\*E-mail: Rainer.Jordan@tu-dresden.de.

### Author Contributions

The manuscript was written through contributions of all authors. All authors have given approval to the final version of the manuscript.

### Notes

The authors declare no competing financial interest.

## ACKNOWLEDGMENTS

This work was supported by grant from the Deutsche Forschungsgemeinschaft (FZ 111) (S.P.) and from the Cluster of Excellence Center for Regenerative Therapies Dresden (CRTD) Seed Grant program (R.J. and S.P.). R.J. acknowledges additional support by the National Institutes of Health through the National Cancer Institute Alliance for Nanotechnology in Cancer (UO1 CA151806). E.M. acknowledges the support from KU Leuven and the Erasmus master program.

## ABBREVIATIONS

CAN, acetonitrile; TEA, triethylamine; PMeOx, poly(2-methyl-2-oxazoline); POx, poly(2-oxazoline); HEMA, (hydroxyethyl)-methacrylate; METAC, 2-methacryloxyethyltrimethylammonium; PAH, poly(allylaminehydrochloride); PSS, poly(sodium-4-styrene-sulfonate); PNIPAAm, poly(*N*-isopropylacrylamide); dH<sub>2</sub>O, deionized water; PLL, poly(L-lysine); DMSO, dimethyl sulfoxide; BSA, bovine serum albumin; DPBS, Dulbecco's phosphate-buffered saline; FITC, fluorescein isothiocyanate; HEK, human embryonic kidney; DMEM, Dulbecco's Modified Eagle Medium; bFGF, basic fibroblast growth factor; PBS, phosphate buffered saline; NPC, neuronal progenitor cell; NGS, normal goat serum; MGP, microgel particle

## REFERENCES

- (1) Staudinger, H.; Husemann, E. On highly polymeric compounds, 116(th) Announcement - On the limite swellable poly-styrene. *Ber. Dtsch. Chem. Ges.* **1935**, *68*, 1618–1634.
- (2) Bradna, P.; Stern, P.; Quadrat, O.; Snparek, J. Thickening effect of dispersions of ethyl acrylate–methacrylic acid copolymer prepared by different polymerization routes. *Colloid Polym. Sci.* **1995**, *273* (4), 324–330.
- (3) Sasa, N.; Yamaoka, T. Surface-activated photopolymer microgels. *Adv. Mater.* **1994**, *6* (5), 417–421.
- (4) Vinogradov, S. V. Colloidal microgels in drug delivery applications. *Curr. Pharm. Des.* **2006**, *12* (36), 4703–4712.
- (5) Lee, Y.; Park, S. Y.; Kim, C.; Park, T. G. Thermally triggered intracellular explosion of volume transition nanogels for necrotic cell death. *J. Controlled Release* **2009**, *135* (1), 89–95.
- (6) Tan, J. P. K.; Goh, C. H.; Tam, K. C. Comparative drug release studies of two cationic drugs from pH-responsive nanogels. *Eur. J. Pharm. Sci.* **2007**, *32* (4–5), 340–348.
- (7) Liu, Y. Y.; Shao, Y. H.; Lu, J. Preparation, properties and controlled release behaviors of pH-induced thermosensitive amphiphilic gels. *Biomaterials* **2006**, *27* (21), 4016–4024.
- (8) Kim, J.; Nayak, S.; Lyon, L. A. Bioresponsive hydrogel microlenses. *J. Am. Chem. Soc.* **2005**, *127* (26), 9588–9592.

- (9) Guan, Y.; Zhang, Y. J. PNIPAM microgels for biomedical applications: from dispersed particles to 3D assemblies. *Soft Matter* **2011**, *7* (14), 6375–6384.

- (10) Wheeldon, I.; Ahari, A. F.; Khademhosseini, A. Microengineering Hydrogels for Stem Cell Bioengineering and Tissue Regeneration. *Jala* **2010**, *15* (6), 440–448.

- (11) Gan, T. T.; Guan, Y.; Zhang, Y. J. Thermogelable PNIPAM microgel dispersion as 3D cell scaffold: effect of syneresis. *J. Mater. Chem.* **2010**, *20* (28), 5937–5944.

- (12) Dargaville, T. R.; Forster, R.; Farrugia, B. L.; Kempe, K.; Voorhaar, L.; Schubert, U. S.; Hoogenboom, R. Poly(2-oxazoline) hydrogel monoliths via thiol-ene coupling. *Macromol. Rapid Commun.* **2012**, *33* (19), 1695–1700.

- (13) Chu, L. Y.; Utada, A. S.; Shah, R. K.; Kim, J. W.; Weitz, D. A. Controllable monodisperse multiple emulsions. *Angew. Chem., Int. Ed. Engl.* **2007**, *46* (47), 8970–4.

- (14) Dendukuri, D.; Hatton, T. A.; Doyle, P. S. Synthesis and self-assembly of amphiphilic polymeric microparticles. *Langmuir* **2007**, *23* (8), 4669–74.

- (15) Bong, K. W.; Pregibon, D. C.; Doyle, P. S. Lock release lithography for 3D and composite microparticles. *Lab Chip* **2009**, *9* (7), 863–6.

- (16) Acharya, G.; Shin, C. S.; McDermott, M.; Mishra, H.; Park, H.; Kwon, I. C.; Park, K. The hydrogel template method for fabrication of homogeneous nano/microparticles. *J. Controlled Release* **2009**, *141* (3), 314–9.

- (17) Lewis, C. L.; Lin, Y.; Yang, C.; Manocchi, A. K.; Yuet, K. P.; Doyle, P. S.; Yi, H. Microfluidic fabrication of hydrogel microparticles containing functionalized viral nanotemplates. *Langmuir* **2010**, *26* (16), 13436–41.

- (18) Chapin, S. C.; Pregibon, D. C.; Doyle, P. S. High-throughput flow alignment of barcoded hydrogel microparticles. *Lab Chip* **2009**, *9* (21), 3100–9.

- (19) Pautot, S.; Wyart, C.; Isacoff, E. Y. Colloid-guided assembly of oriented 3D neuronal networks. *Nat. Methods* **2008**, *5* (8), 735–40.

- (20) Jgamadze, D.; Bergen, J.; Stone, D.; Jang, J. H.; Schaffer, D. V.; Isacoff, E. Y.; Pautot, S. Colloids as mobile substrates for the implantation and integration of differentiated neurons into the mammalian brain. *PLoS One* **2012**, *7* (1), e30293.

- (21) Jgamadze, D.; Liu, L.; Vogler, S.; Chu, L. Y.; Pautot, S. Thermoswitching microgel carriers improve neuronal cell growth and cell release for cell transplantation. *Tissue Eng., Part C* **2015**, *21* (1), 65–76.

- (22) Hynd, M. R.; Turner, J. N.; Shain, W. Applications of hydrogels for neural cell engineering. *J. Biomater. Sci. Polym. Ed* **2007**, *18* (10), 1223–44.

- (23) Aoi, K.; Okada, M. Polymerization of oxazolines. *Prog. Polym. Sci.* **1996**, *21* (1), 151–208.

- (24) Cesana, S.; Auernheimer, J.; Jordan, R.; Kessler, H.; Nuyken, O. First poly(2-oxazoline)s with pendant amino groups. *Macromol. Chem. Phys.* **2006**, *207* (2), 183–192.

- (25) Taubmann, C.; Luxenhofer, R.; Cesana, S.; Jordan, R. First aldehyde-functionalized poly(2-oxazoline)s for chemoselective ligation. *Macromol. Biosci.* **2005**, *5* (7), 603–612.

- (26) Cesana, S.; Kurek, A.; Baur, M. A.; Auernheimer, J.; Nuyken, O. Polymer-bound thiol groups on poly(2-oxazoline)s. *Macromol. Rapid Commun.* **2007**, *28* (5), 608–615.

- (27) Levy, A.; Litt, M. Polymerization of cyclic iminoethers 0.5. 1,3-Oxazolines with hydroxy- acetoxy- and carboxymethyl-alkyl groups in 2 position and their polymers. *J. Polym. Sci., Part A-1: Polym. Chem.* **1968**, *6* (7PA1), 1883.

- (28) Luxenhofer, R.; Jordan, R. Click chemistry with poly(2-oxazoline)s. *Macromolecules* **2006**, *39* (10), 3509–3516.

- (29) Persigehl, P.; Jordan, R.; Nuyken, O. Functionalization of amphiphilic poly(2-oxazoline) block copolymers: A novel class of macroligands for micellar catalysis. *Macromolecules* **2000**, *33* (19), 6977–6981.

(30) Luxenhofer, R.; Bezen, M.; Jordan, R. Kinetic investigations on the polymerization of 2-oxazolines using pluritriplate initiators. *Macromol. Rapid Commun.* **2008**, *29* (18), 1509–1513.

(31) Zhang, N.; Huber, S.; Schulz, A.; Luxenhofer, R.; Jordan, R. Cylindrical molecular brushes of poly(2-oxazoline)s from 2-isopropenyl-2-oxazoline. *Macromolecules* **2009**, *42* (6), 2215–2221.

(32) Kelly, A. M.; Wiesbrock, F. Strategies for the synthesis of poly(2-oxazoline)-based hydrogels. *Macromol. Rapid Commun.* **2012**, *33* (19), 1632–1647.

(33) Hartlieb, M.; Kempe, K.; Schubert, U. S. Covalently cross-linked poly(2-oxazoline) materials for biomedical applications – From hydrogels to self-assembled and templated structures. *J. Mater. Chem. B* **2015**, *3* (4), 526–538.

(34) Hoogenboom, R. Poly(2-oxazoline)s: A polymer class with numerous potential applications. *Angew. Chem., Int. Ed.* **2009**, *48* (43), 7978–7994.

(35) Legros, C.; De Pauw-Gillet, M. C.; Tam, K. C.; Lecommandoux, S.; Taton, D. pH and redox responsive hydrogels and nanogels made from poly(2-ethyl-2-oxazoline). *Polym. Chem.* **2013**, *4* (17), 4801–4808.

(36) Einzmann, M.; Binder, W. H. Novel functional initiators for oxazoline polymerization. *J. Polym. Sci., Part A: Polym. Chem.* **2001**, *39* (16), 2821–2831.

(37) Viegas, T. X.; Bentley, M. D.; Harris, J. M.; Fang, Z. F.; Yoon, K.; Dizman, B.; Weimer, R.; Mero, A.; Pasut, G.; Veronese, F. M. Polyoxazoline: Chemistry, properties, and applications in drug delivery. *Bioconjugate Chem.* **2011**, *22* (5), 976–986.

(38) Luxenhofer, R.; Schulz, A.; Roques, C.; Li, S.; Bronich, T. K.; Batrakova, E. V.; Jordan, R.; Kabanov, A. V. Doubly amphiphilic poly(2-oxazoline)s as high-capacity delivery systems for hydrophobic drugs. *Biomaterials* **2010**, *31* (18), 4972–9.

(39) Viegas, T. X.; Bentley, M. D.; Harris, J. M.; Fang, Z.; Yoon, K.; Dizman, B.; Weimer, R.; Mero, A.; Pasut, G.; Veronese, F. M. Polyoxazoline: chemistry, properties, and applications in drug delivery. *Bioconjugate Chem.* **2011**, *22*, 976–986.

(40) Pidhatika, B.; Rodenstein, M.; Chen, Y.; Rakhmatullina, E.; Muhlebach, A.; Acikgoz, C.; Textor, M.; Konradi, R. Comparative stability studies of poly(2-methyl-2-oxazoline) and poly(ethylene glycol) brush coatings. *Biointerphases* **2012**, *7*, 1–4.

(41) Ulbricht, J.; Jordan, R.; Luxenhofer, R. On the biodegradability of polyethylene glycol, polypeptoids and poly(2-oxazoline)s. *Biomaterials* **2014**, *35* (17), 4848–4861.

(42) Gaertner, F. C.; Luxenhofer, R.; Blechert, B.; Jordan, R.; Essler, M. Synthesis, biodistribution and excretion of radiolabeled poly(2-alkyl-2-oxazoline)s. *J. Controlled Release* **2007**, *119* (3), 291–300.

(43) Lück, S.; Schubel, R.; Mathieu, E.; Zimmermann, H.; Scharnweber, D.; Pautot, S.; Jordan, R. Submitted for publication to *Biomaterials*, 2014 (under revision).

(44) Frey, M. T.; Engler, A.; Discher, D. E.; Lee, J.; Wang, Y. L. Microscopic methods for measuring the elasticity of gel substrates for cell culture: Microspheres, microindenters, and atomic force microscopy. *Method Cell Biol.* **2007**, *83*, 47–65.

(45) Letourneau, P. C. Possible roles for cell-to-substratum adhesion in neuronal morphogenesis. *Dev. Biol.* **1975**, *44* (1), 77–91.

(46) Huber, S.; Jordan, R. Modulation of the lower critical solution temperature of 2-alkyl-2-oxazoline copolymers. *Colloid Polym. Sci.* **2008**, *286*, 395–402.

(47) Park, J. S.; Kataoka, K. Precise control of lower critical solution temperature of thermosensitive poly(2-isopropyl-2-oxazoline) via gradient copolymerization with 2-ethyl-2-oxazoline as a hydrophilic comonomer. *Macromolecules* **2006**, *39*, 6622–6630.